

A QUANTUM CHEMISTRY APPROACH TO THE ELECTRO-OXIDATION OF CO ADSORBED ON Rh(111) CLUSTER SURFACES*

P. PAREDES OLIVERA, G.L. ESTIÚ, E.A. CASTRO and A.J. ARVÍA

*Instituto de Investigaciones Fisicoquímicas Teóricas y Aplicadas (INIFTA),
Facultad de Ciencias Exactas, Universidad Nacional de la Plata, Casilla de Correo 16,
Sucursal 4, (1900) La Plata (Argentina)*

ABSTRACT

A molecular-orbital interpretation of the electro-oxidation of CO adsorbed on Rh(111) single-crystal clusters in the presence of H₂O is described. Calculations were based on the atom superposition and electron delocalization method. Different stabilization energies for ensembles of the type [Me]_N(CO)_n(OH)_m for Me = Rh or Pt are given. The stability of possible CO adsorbate configurations on Rh(111) surfaces depends on the applied electric potential in a way which is directly comparable with the one reported previously for CO adsorbates on Pt(111). Only linearly bonded CO adsorbates appear to be involved in the electrochemical CO oxidative interaction with H₂O molecules on both Rh(111) and Pt(111).

INTRODUCTION

The electronic and molecular structure of the electrochemical interface plays a decisive role in determining the kinetics and the mechanism of processes that occur at electrocatalytic solid surfaces. This matter has been of particular interest in the last decade and it has stimulated the application of surface physico-chemical techniques, either in situ or ex situ, to establish the possible adsorbate structures at the electrochemical interface [1-6]. These studies have recently provided valuable information from the examination of synthetic interfaces [7,8] built up by means of the co-adsorption of carefully selected adsorbates capable of simulating the structure of the adsorbed layer and the effective electrode potential simultaneously.

Co-adsorption studies such as those involving the electro-oxidation of CO adsorbates in acid solution, either hydrophilic on Rh(111) or hydrophobic on Pt(111) electrodes [9], have shown that the corresponding reactants could be described as complex adsorbates resulting from cooperative interactions be-

*Presented at the 18th International Congress of Theoretical Chemists of Latin Expression, held at La Plata, Argentina. 23-28 September, 1989.

tween different species at the electrochemical interface [10,11]. The influence of $(\text{CO})_{\text{ad}}(\text{OH})_{\text{ad}}$ lateral interactions on CO adsorbate electro-oxidation kinetics on Pt(111) has been recently semiempirically evaluated [12] in terms of the stability of the different adsorbate ensembles represented by the general stoichiometry $[\text{Pt}]_N(\text{CO})_n(\text{OH})_m$. In this case the OH co-adsorbate which results from the direct electro-oxidation of H_2O at 0.6 V (vs. RHE) favours that complex adsorbate structure. The stability of those ensembles depends on the value of n and m , and on the applied electric potential. Therefore, it is reasonable to expect that the voltammetric electro-oxidation of CO adsorbed on Pt gives rise to distinguishable electro-oxidation peaks for different CO coverages, as each m/n stoichiometric ratio should be related to a well-defined limit of the stability of the adsorbate ensemble.

In contrast to previous kinetic interpretations which concluded that the position of CO electro-oxidation voltammetric current peaks should be assigned to different CO coordination geometries on Pt, i.e. linearly bonded, bridged and multiply bonded adsorbed CO states, the molecular-orbital (MO) calculations allow it to be concluded that the multiplicity and location of the voltammetric peaks could be reasonably explained through cooperative interactions among preadsorbed OH species and a different number of linearly bonded adsorbed CO molecules on Pt.

The electro-oxidation of CO adsorbed on Rh in acid solutions has been often compared with the reaction occurring on Pt [9,13]. Accordingly, the kinetics of the reaction on Rh has been explained in terms of two distinguishable CO adsorbates, but, in this case, the appearance of a single voltammetric current peak was explained through the interconversion of adsorbed CO from bridge to linear coordination, a process which on Rh was faster than on Pt [13]. In contrast, the binding energies (BE) derived from MO calculations for the electric potential related to CO electro-oxidation, indicate that the linear CO adsorbate configuration on Rh becomes sufficiently stable [14], turning out to the spontaneous change from linear to bridged CO adsorbate rather unlikely. However, the location of the CO adsorbate electro-oxidation peak on Rh is highly dependent on the electrolyte solution composition [13,15,16,28,29]. The CO adsorbate electro-oxidation voltammetric peak on Rh in acid media (1 M HClO_4 , 0.5 M H_2SO_4) appears at about 0.75 V [15,16], whereas in neutral 0.2 M K_2SO_4 it is found at 0.95 V. However, a single voltammetric peak at 0.95 V was recorded in 1.0 M HClO_4 after the CO monolayer surface coverage had been attained [13].

This paper is devoted to a MO-based description of CO adsorbate electro-oxidation on Rh(111) in the presence of H_2O . The results can be used to interpret the corresponding electrochemical data available at present in the literature [13,15,16]. The calculation procedure, which has been described in an earlier publication [14], is based on the existence of strong lateral interactions between CO and H_2O , CO and OH, and COH and OH co-adsorbates on Rh(111)

clusters under different applied electric potentials. Both H_2O and CO form a stable co-adsorbate on $\text{Rh}(111)$ already at 0.0 V vs. the reversible hydrogen electrode (RHE). Then, both the $\text{H}_2\text{O}\text{-CO}$ or $\text{CO}\text{-OH}$ lateral interactions extend over the entire potential range where bulk H_2O becomes thermodynamically stable [9,14]. The characteristics of these interactions change considerably with both the applied electric potential and the solution composition.

OUTLINE OF THE CALCULATION PROCEDURE

In a previous paper [14] atom-superposition and electron-delocalization (ASED-MO) calculations [17,18] were employed for modelling the CO -adsorbate configurations on a $\text{Rh}(111)$ cluster surface as a function of the applied electric potential. The same procedure was employed in the present study to describe the changes in the $\text{CO}\text{-H}_2\text{O}$ adsorbate structure on $\text{Rh}(111)$ as the applied electric potential is set increasingly positive to reach the region where the CO electro-oxidation reaction begins.

The $\text{Rh}(111)$ surface was built up from $[\text{Rh}]_{22}$ high-spin bulk superimposable clusters as described in Ref. 14 for the same geometric parameters (Fig. 1). This is the smallest cluster dimension which minimizes border effects when cooperative interactions between adsorbates on the central four-atom-cluster region are considered (Fig. 2). The parameters which define the uncharged $[\text{Rh}(111)]_{22}(\text{H}_2\text{O})_m(\text{CO})_n$ adsorbed ensemble were taken from Ref. 14 and, due to the invariance of $\text{Rh}\text{-O}$ charge transfer on the metal surface, these parameters remained unchanged when adsorbed H_2O was replaced by OH adsorbate (Table 1).

Both CO [11,12,23] and OH [11,24] species adsorb in a linear configuration perpendicular to the metal surface. The $\text{C}\text{-O}$ and $\text{O}\text{-H}$ interatomic distances were fixed at 1.16 and 1.00 Å, respectively. The OH adsorbate is located 1.95 Å from the $\text{Rh}(111)$ surface and 2.0 Å from the $\text{Pt}(111)$ surface, whereas the CO adsorption distances were 1.95 for $\text{Rh}(111)$ and 2.00 Å for $\text{Pt}(111)$. The

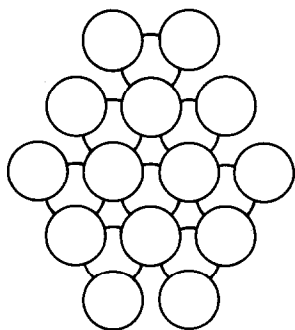


Fig. 1. Cluster used to model the $[\text{Rh}(111)]_{22}$ surface structure.

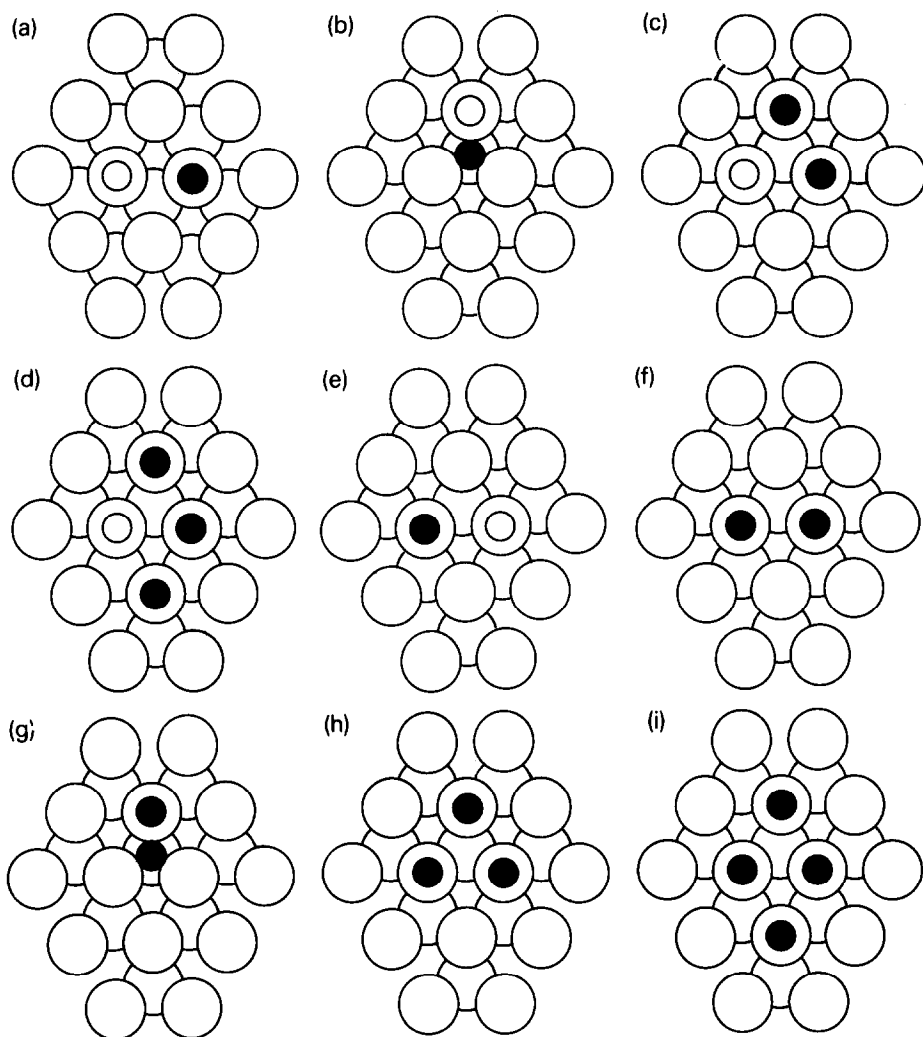


Fig. 2. Local structures involving the central atoms of the cluster. The energy of the various configurations are compared in order to define the stability inversion potential (SIP) on Rh(111). Comparisons are of structures a and f, b and g, c and h, d and g, and e and f. (○) OH; (●) CO; (●) COH (in Fig. 2 (e)).

metal–O bonding for OH adsorption implies an ionic character (charge transfer). The adsorption bond lengths were calculated from the corresponding minimum energy value. They are directly related to the sum of the corresponding atomic radii. In contrast to the fact that covalent radii are almost the same for Rh and Pt, the ionic radii for Rh is 65% larger than that for Pt. This difference is reflected in the C–metal adsorption bond length which, in the presence of co-adsorbed OH, is 0.19 Å longer for Rh than for Pt. This means that

TABLE 1

Parameters used in the calculations: principal quantum number (n), orbital exponents (ζ), ionization potential (VSIP) and the corresponding coefficients (C_1 and C_2) for d orbitals

Atom ^a		s			p		
		n	ζ	VSIP	n	ζ	VSIP
O	(A)	2	1.946	-26.98	2	1.927	-12.12
	(B)	2	2.146	-26.98	2	2.127	-12.12
H	(A)	1	1.000	-12.10			
C	(B)	2	1.658	-18.50	2	1.618	-9.760
	(C)	5	2.135	-9.670	5	2.100	-6.314
d							
		n	ζ_1	VSIP	C_1	C_2	ζ_2
Rh	(C)	4	4.290	-11.77	0.5807	0.5685	1.970

^a(A) Atom in H₂O molecule; (B) atom in CO molecule; (C) Rh in the [Rh(111)]₁₉(OH) _{n} (CO) _{m} system.

for the co-adsorbed ensemble the Rh-C bond length increases from 1.95 to 2.24 Å.

In order to simulate positive applied electric potentials (positive charging) valence state ionization potential (VSIP) values were decreased (increased in absolute value) from those which define the zero potential condition. In previous studies related to CO adsorbates on Rh(111) [14] changes of ± 1.0 eV in VSIP have been correlated to changes of ± 1.0 V from the zero potential. In this way the correct trend in the CO adsorption-geometry change with the applied electric potential was accomplished. When the CO electro-oxidation on Pt(111) was considered [12], a 1.0 V shift in the applied potential was correlated to a 0.32 eV shift in the corresponding Fermi energy level. This energy-scale adjustment gave very good agreement between the position of the various CO voltammetric electro-oxidation peaks on Pt in acid and the stabilization energies of the different Pt(CO)·Pt(OH) adsorbate ensembles. A similar correlation emerged for the CO voltammetric electro-oxidation peaks on Rh(111) provided that the energy scale (linear work function vs. applied electric potential correlation) is adjusted to 0.3 eV V⁻¹. The fact that the behaviour of CO adsorbates on Pt(111) and Rh(111) is similar indicates that both types of adsorbate "feel" about 30% of the entire potential drop applied to the metal/solution interface, in agreement with the experimental findings for the CO-Pt(111) interface [19].

It should be noted that the one-to-one correlation between the work function in an electrochemical environment and the applied electric potential, derived

from ESCA data for Au electrodes immersed in a cesium halide containing solution [1,20], has been extended to interpret data of other systems [14,21]. In contrast, the shift in Fermi energy level with the applied electric potential differs appreciably for various metal/electrolyte interfaces, as expected, because the characteristics of this correlation is determined by both surface and bulk state energies, which in turn exhibit specific responses to the applied electric potential. A 0.3-eV shift in surface state energy was measured for a 1.0-V shift in the energy of bulk states for the Au(100)/0.5 M NaF system, whereas slopes ranging between 3 and 4 eV/V were observed for the Ag(110)/0.5 M NaF interface [22].

The influence of surface-state concentration on the adsorbate behaviour at solid electrode surfaces explains the 0.3 eV V^{-1} slope for the correlation between the CO electro-oxidation peak potentials (in volt) and the stability energy of the Rh(CO)·Rh(OH) co-adsorbates (in eV) calculated for different Fermi level energy values.

RESULTS AND INTERPRETATION

Structural aspects

For a molecular-level interpretation of the present results and for establishing a correlation between theory and experimental data it is convenient to consider the results obtained previously for Pt(111) [12]. The interpretation of CO adsorbate electro-oxidation voltammetric data on Rh and Pt electrodes in acids has been based upon the same type of interactions [13], despite the fact that the reaction exhibits two voltammetric current peaks on Pt [15,25,27], but a single peak on Rh [13,14,28,29], the location of the latter being dependent on the electrolyte composition and pH [16].

The appearance of a single voltammetric peak for the adsorbate electro-oxidation on Rh has been explained through an energy difference of the linear and bridge CO adsorbates on Rh smaller than that resulting for the same species on Pt, i.e. the interconversion from "bridge" to "linear" CO adsorbate on Rh becomes considerably more facile [13] than on Pt. However, this interpretation can hardly be supported through MO calculations [14], as in this case a similar BE difference between bridged and linearly bonded CO on both Pt(111) and Rh(111) surfaces is obtained. However, it should be noted that the interconversion mechanism offers no explanation for the pH dependence of the CO adsorbate electro-oxidation peak potential on Rh. It was found that CO displaces H atoms from Rh with great difficulty [13,30], so that a complete CO monolayer in acid solutions can hardly be obtained. Nevertheless, after a prolonged adsorption time the CO adsorbate electro-oxidation voltammogram on Rh becomes independent of the solution pH [13]. Furthermore, in contrast to the interconversion mechanism, the MO calculation indicates that

the H adatom concentration remaining on the Rh surface after CO adsorbate formation determines the location of the CO electro-oxidation peaks through their occupancy of surface sites.

As it has been previously reported for Pt(111) [12], CO adsorbate electro-oxidation on Rh(111) can be also described through the stability of the different $[\text{Rh}(111)]_{22}(\text{CO})_n(\text{OH})_m$ ensembles on the basis of possible stages participating in the CO adsorbate electro-oxidation [27]. This sequence of stages can be compared more critically with the interconversion mechanism derived from voltammetry data, by considering the influence of the applied electric potential on the stability of the different adsorbate ensembles.

In addition to the $[\text{Rh}(111)]_{22}(\text{OH})(\text{CO})$ and $[\text{Rh}(111)]_{22}(\text{H}_2\text{O})(\text{CO})$ ensembles formed on the Rh(111) uncharged surface [14], other configurations such as the $[\text{Rh}(111)]_{22}(\text{COH})(\text{OH})$ one, which may result from a chemical reaction at the surface level can also be considered. For a certain applied electric potential, oxidative interactions yielding CO_2 as product leave a $[\text{Rh}(111)]_{22}(\text{CO})_{n+m}$ ensemble, the formation of which becomes more favourable than that of the CO-OH, CO-H₂O or the COH-OH co-adsorbed structure [12,28].

Although the true structure of the Rh(111)/electrolyte solution interface in the presence of CO adsorbates cannot be described exactly, a reasonable picture of the adsorbate structures resulting for different CO surface coverages can be envisaged from the Rh/CO(gas) interface spectroscopic data [30-32]. Thus, at low CO surface coverages, a $(\sqrt{3} \times \sqrt{3})R$ 30° LEED pattern is produced through the CO occupancy of Rh(111) top sites (Fig. 3). This structure gives rise to the CO·OH interactions depicted in Fig. 2(a). Otherwise, at high CO surface coverages, the simultaneous occupancy of Rh(111) top and hollow sites results in a $c(2 \times 2)$ LEED pattern (Fig. 4). The possible interactions between the co-adsorbed CO and OH species in this case are illustrated in Figs. 2(a-c). The structure depicted in Fig. 2(c) is formed under a positive applied

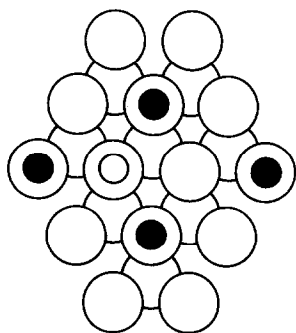


Fig. 3. The $(\sqrt{3} \times \sqrt{3})R$ 30° LEED pattern corresponding to CO adsorbed on Rh(111) for $\theta = 0.33^\circ$ [31]. The possible OH adsorption site is also included. The structure of the adsorbed layer remains on the application of a positive potential.

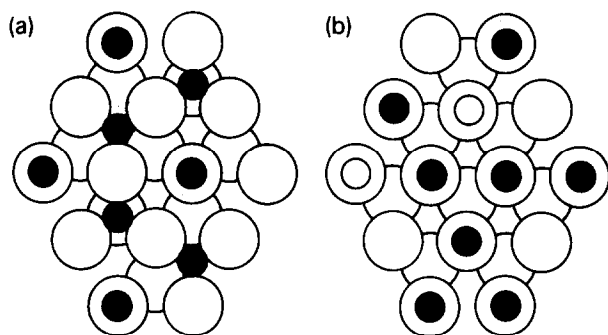


Fig. 4. (a) Adsorbed structure as derived from the $c(2 \times 2)$ LEED pattern of CO adsorbed on the Rh(111) uncharged surface for $\theta = 0.5^\circ$ [31,32]. The OH adsorption site is also included. (b) Adsorbed structures resulting from the application of a positive potential to the initial $c(2 \times 2)$ structure. ●, CO; ○, OH.

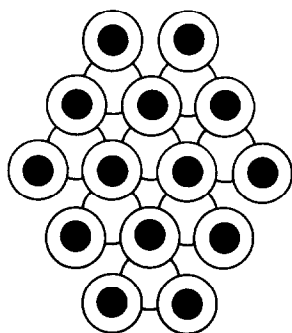


Fig. 5. Adsorbed structure for $\theta = 1.0^\circ$ and a positive applied potential. A local $(\text{CO})_{\text{ad}}$ vacancy is necessary for OH adsorption. ●, CO.

electric potential (positive charging) which assists the shift of the CO adsorbate from a highly to singly coordinated Rh(111) site [14]. Unfortunately, there is no information concerning adsorbate structures at higher CO surface coverages on the Rh/CO(gas) interface, although calculations show that for positive applied electric potentials, an adsorbate structure such as that depicted in Fig. 5, could be obtained through the type of interaction depicted in Fig. 2(d). However, the CO-H₂O coadsorbate may also undergo a chemical reaction yielding the COH·OH structure shown in Fig. 2(e).

The energy of the co-adsorbed structures represented in Figs. 2(a)–(e) changes continuously as the potential increases from 0.0 to 1.0 V, and becomes gradually more labile than those depicted in Figs. 2(f)–2(i). Hence, on the basis of these results, it is possible to define a stability inversion potential (SIP) at which the structure containing two different interacting near-neighbour adsorbate units, either CO–OH or COH–OH, change into a new adsorbate structure built up by means of adsorbed CO, and leading to CO₂ production.

The SIP values related to the different adsorbate configurations can be correlated directly with the potentials of the various voltammetric peaks for the electro-oxidation to CO_2 of CO adsorbed on Rh(111) in aqueous solution [13,15,16]. Thus, according to data assembled in Table 2 the voltammetric peak at 0.95 V can be assigned to the electro-oxidation threshold potential for the rupture of the $(\text{CO})_3(\text{OH})$ adsorbate ensemble (Fig. 2(d)). The $(\text{CO})_3(\text{OH})$ ensemble should be produced at CO surface coverages approaching the monolayer value. It should be noted that in this case the electro-oxidation voltammogram shows a shoulder at 0.75 V appearing together with the peak at 0.95 V [13]. On the basis that CO hardly displaces H adatoms from the Rh surface, it sounds reasonable that under these circumstances in acid solutions, co-adsorbate interactions such as those depicted in Fig. 2(c) are involved, as the fourth adsorption site on Rh(111) is then occupied by a H atom. Accordingly, depending on the solution pH, the voltammetric electro-oxidation peak of CO adsorbates on Rh(111) for a relatively prolonged adsorption time would appear at either 0.95 or 0.75 V.

Otherwise, for low CO surface coverage and linear CO adsorbate coordination assisted through a positive charging, the rupture of the resulting $(\text{CO})_2(\text{OH})$ ensemble (Fig. 2(c)) would give rise to the electro-oxidation peak at 0.75 V. The latter can be also seen for high CO surface coverages in acid electrolyte solutions.

The CO-OH interactions resulting for the structure depicted in Fig. 2(a), prevailing at low CO surface coverages, would produce a voltammetric electro-

TABLE 2

Correlation between SIP values (expressed as $H_{6.56eRh}$) and the voltammetric peak potentials related to the electro-oxidation of different CO adsorbates on Rh(111)^a

Adsorbate on $[\text{Rh}(111)]_{22}$	Electro-oxidation potential (V)	SIP ^b (eV)	CBE ^c (eV)
$(\text{CO})(\text{OH})/(\text{CO})_2$ Fig. 2(a) and 2(f)	0.47	-9.81	7.36
$(\text{CO})_2(\text{OH})/(\text{CO})_3$ Fig. 2(b) and 2(g)	0.75	-9.89	5.48
$(\text{CO})_3(\text{OH})/(\text{CO})_4$ Fig. 2(c) and 2(h)	0.95	-9.95	3.66
$(\text{CO})^{\text{H}}(\text{OH})^{\text{T}}/(\text{CO})^{\text{H}}(\text{CO})^{\text{T}}$ Fig. 2(d) and 2(i)	1.62	-10.15	3.14

^aThe values given in the table indicate the possible adsorbed structures which give rise to the voltammetric CO electro-oxidation peaks on Rh in aqueous solutions when the 0.3 eV V^{-1} correlation is used. ^bSIP are expressed as ionization-potential values of the Rh(111) surface, i.e. the way in which electrode charging was simulated. ^cCo-adsorption BE (CBE) values calculated at the SIP value of each structure: $\text{CBE} = E_{[\text{Rh}(111)]_{22}(\text{CO})_n(\text{OH})_m} - E_{[\text{Rh}(111)]_{22}} - nE_{\text{CO}} - mE_{\text{OH}}$.

oxidation peak at 0.47 V, which would be observed on Rh(111) at low CO surface coverage. This peak has not been observed experimentally. Nevertheless, providing that in this case the influence of the applied electric potential on the adsorbate structure becomes sufficiently small, the (CO)(OH) co-adsorbate can originate several new configurations such as those depicted in Fig. 2(b), which in turn become less stable than that shown in Fig. 2(g). Likewise, sufficiently large positive charging can change the adsorbate structure from that shown in Fig. 2(b) into that illustrated in Fig. 2(a).

The co-adsorption of H₂O and CO on Rh(111) at zero potential can also produce the structure depicted in Fig. 2(e) through a surface reaccommodation reaction [9]. The resulting unstable adsorbate would also be electro-oxidized at a relatively low potential, which in this case is in the potential range of the hydrogen evolution reaction. In this case the unstable (OH)_{ad} species on Rh(111) would result exclusively from a surface chemical reaction. Nevertheless, all these unstable structures, which have only been deduced theoretically, are excluded from Table 2.

Molecular orbital interpretation

Cooperative interactions resulting from co-adsorbed CO and OH on Rh(111) can be described in the basis of MO interactions involving CO and OH adsorption on transition-metal surfaces [12,23,24]. It should be noted that H₂O electrodecomposition yielding adsorbed OH and H⁺ ions on Rh in acid solution begins at a potential at which the Rh(111) surface is already mostly covered by linearly bonded CO adsorbate.

The stabilization of OH orbitals through bonding interactions occurs similarly on both the [Rh(111)]₂₂(CO)_n and [Rh(111)]₂₂ substrates. However, perturbative interactions involving OH and preadsorbed CO increase the energy of the antibonding Rh(OH) orbital levels, a fact which explains why OH becomes more strongly bonded to the metal as *n*, the number of CO molecules in the adsorbate ensemble, increases. Thus, for a given applied electric potential and metal surface structure (Fig. 6), a comparison of the adsorptive stabilization energies for OH on [Rh(111)]₂₂, [Rh(111)]₂₂(CO), [Rh(111)]₂₂(CO)₂ and [Rh(111)]₂₂(CO)₃ indicates an increasing stability of the co-adsorbate ensemble produced by the less effective OH antibonding interaction.

However, the Fermi energy level of Rh decreases with positive applied electric potentials (positive charging). Accordingly, the stability of co-adsorbate ensembles decreases on increasing the strength of the antibonding interactions, leading to their desorption as CO₂ and H⁺ in solution when the corresponding threshold potential value is reached. Therefore, a definite threshold potential value can be associated with the electro-oxidation-desorption condition of each particular adsorbate ensemble on the Rh(111) substrates. The

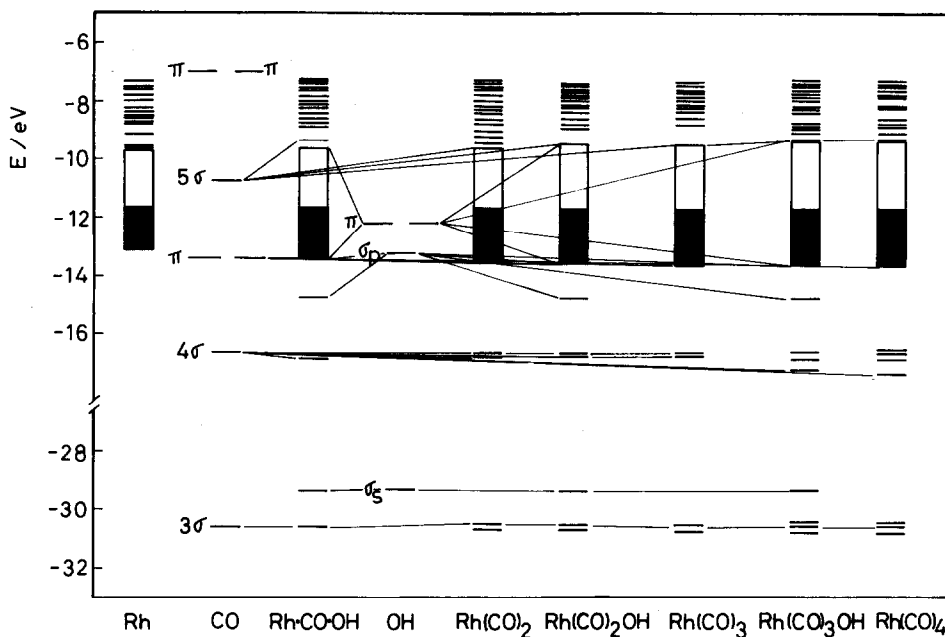


Fig. 6. Molecular-orbital correlation diagrams for the adsorption of $(\text{CO})_n$ ($0 \leq n \leq 3$) and (OH) on $\text{Rh}(111)$.

greater the CO surface coverage the higher the applied electric potential required for the adsorbate electro-oxidative desorption.

CONCLUSIONS

Semiempirical ASED-MO calculations provide the basis for a structural interpretation of adsorbed CO electro-oxidation reaction on $\text{Rh}(111)$ single-crystal clusters in the presence of H_2O .

The appearance of a single voltammetric electro-oxidation peak, which is observed after a sufficiently prolonged CO adsorption time, that is, for a Rh surface nearly completely covered by CO, has been explained through the facile interconversion of multiply bonded CO adsorbates into linearly bonded ones on the Rh surface [13,18]. The peak position depends on electrolyte composition [13,15,16].

According to the present MO calculations, the single electro-oxidation peak at 0.95 V resulting for $\text{Rh}(111)$ obtained in neutral solutions when the monolayer CO surface coverage has been closely attained, results from cooperative interactions involving OH species co-adsorbed with a relatively large number of linearly bonded CO molecules.

As the Rh surface sites begin to be occupied by H adatoms in acid electrolytes

[15,16], the complete CO surface coverage monolayer cannot be achieved, resulting in the displacement of the CO electro-oxidation peak to a lower potential (0.75 V). Therefore, under controlled CO exposure time and adsorption potential conditions, it is possible to observe, also in acid solutions, the main CO electro-oxidation voltammetric peak on Rh(111) expected at 0.95 V accompanied by a shoulder at 0.75 V [13]. This result is consistent with the fact that under these conditions H adatoms are almost completely displaced from the Rh(111) surface by CO adsorbates.

Calculations indicate that CO adsorbed structures implying formyl radicals can be also present on the uncharged Rh surface. This type of adsorbate can be detected through the CO vibrational frequency shift for H₂O co-adsorption [9]. However, it is rather unlikely that adsorbed formyl radicals contribute to the voltammetric electro-oxidation of CO on Rh(111) because these adsorbed species are unstable at the potential at which they should be detected. The latter lies within the hydrogen electrode reaction potential range.

The voltammetric electro-oxidation of CO adsorbates on both Rh(111) and Pt(111) [13–16,25–29] takes place at a potential sufficiently positive to allow the kinetics of the process to be assigned principally to an interconversion of CO adsorbates by shifting the adsorbed CO species to on-top Rh surface sites. According to the MO calculations the multiplicity of electro-oxidation peaks can be related to the number of adsorbed CO molecules which are involved in cooperative interactions producing definite stable adsorbate ensembles on Rh(111) at certain well-defined potential ranges. Then, the number of CO molecules in the adsorbate ensemble determines the stability of the entire adsorbate system and, accordingly, the threshold potential for the CO adsorbate oxidative electrodesorption.

ACKNOWLEDGEMENT

The present work was supported by the Consejo Nacional de Investigaciones Científicas y Técnicas and the Comisión de Investigaciones Científicas de la Pcia. de Buenos Aires.

REFERENCES

- 1 E. Kölz, H. Neff and K. Müller, *J. Electroanal. Chem.*, 215 (1986) 33.
- 2 E. Yeager, *Surf. Sci.*, 101 (1980) 1.
- 3 D. Scherson, B. Yao, E. Yeager, J. Eldridge, M. Kordesch and R. Hoffmann, *J. Electroanal. Chem.*, 150 (1986) 535.
- 4 R. Kötz, J. Grobecht, S. Stucki and R. Pixley, *Electrochim. Acta*, 31 (1986) 169.
- 5 W. Hansen, D. Kolb, D. Rath and R. Wille, *J. Electroanal. Chem.*, 110 (1980) 369.
- 6 D. Rath and D. Kolb, *Surf. Sci.*, 109 (1981) 641.
- 7 F. Wagner and T. Moylan, *Surf. Sci.*, 206 (1988) 187.

- 8 F. Wagner and T. Moylan, *Surf. Sci.*, 182 (1987) 125.
- 9 F. Wagner, T. Moylan and S. Schimieg, *Surf. Sci.*, 195 (1988) 403.
- 10 S. Bilmes, M.C. Giordano and A. Arvía, *J. Electroanal. Chem.*, 2215 (1987) 183.
- 11 S. Bilmes, M.C. Giordano and A. Arvía, *Canadian J. Chem.*, 66 (1988) 2259.
- 12 G. Estiú, S. Maluendes, E. Castro and A. Arvía, *J. Electroanal. Chem.*, 283 (1990) 303.
- 13 S. Bilmes, N. Tacconi and A. Arvía, *J. Electroanal. Chem.*, 143 (1983) 179.
- 14 P. Paredes Olivera, G. Estiú, E. Castro and A. Arvía, *J. Mol. Struct. (Theochem)*, submitted.
- 15 B. Beden, A. Bewick, K. Kunimatsu and C. Lamy, *J. Electroanal. Chem.*, 142 (1982) 345.
- 16 K. Kunimatsu, R.O. Lezna and M. Enyo, *J. Electroanal. Chem.*, 258 (1989) 115.
- 17 A. Anderson, *J. Chem. Phys.*, 62 (1975) 1187.
- 18 A. Anderson, R. Grimes and S. Hong, *J. Phys. Chem.*, 91 (1987) 4242.
- 19 S. Holloway and J.K. Noskov, *J. Electroanal. Chem.*, 161 (1984) 193.
- 20 D. Kolb, D. Rath, R. Wille and W. Hansen, *Ber. Bunsenges Phys. Chem.*, 87 (1983) 1108.
- 21 S. Mehandru and A. Anderson, *J. Phys. Chem.*, 93 (1989) 2044.
- 22 W. Boeck and D. Kolb, *Surf. Sci.*, 118 (1982) 613.
- 23 S. Ishi, Y. Ohno and B. Viswanathan, *Surf. Sci.*, 161 (1985) 349.
- 24 A. Anderson, *Surf. Sci.*, 105 (1981) 159.
- 25 J. Léger, B. Beden, C. Lamy and S. Bilmes, *J. Electroanal. Chem.*, 170 (1984) 305.
- 26 B. Beden, S. Bilmes, C. Lamy and J. Léger, *J. Electroanal. Chem.*, 149 (1983) 295.
- 27 S. Bilmes and A. Arvia, *J. Electroanal. Chem.*, 198 (1986) 137.
- 28 F. Hahn, B. Beden and C. Lamy, *J. Electroanal. Chem.*, 204 (1986) 315.
- 29 S. Bilmes, Ph.D. thesis, University of Buenos Aires, 1982.
- 30 G. Padyukova, A. Fasman and I. Khizhliniyak, *Electrokhimiya*, 4 (1968) 194.
- 31 P. Thiel, E. Williams, J. Yates and W. Weinberg, *Surf. Sci.*, 84 (1979) 54.
- 32 L. Dubois and G. Somorjai, *Surf. Sci.*, 91 (1980) 514.
- 33 J. Kjöll, T. Ala-Nissila and S. Ying, *Surf. Sci.*, 214 (1989) 448.